Simple Integration of Three-phase Shunt Active Power Filter and Photovoltaic Generation System with Fibonacci-Search-Based MPPT

Hanny H. Tumbelaka [1], Masafumi Miyatake [2]
[1]Department of Electrical Engineering, Petra Christian University, Surabaya, Indonesia
[2]Department of Engineering and Applied Sciences, Sophia University, Tokyo, Japan
E-mail: tumbeh@petra.ac.id

***Abstract* — This paper proposes a three-phase four wire current-controlled Voltage Source Inverter (CC-VSI) for both harmonic mitigation and PV energy extraction. For harmonic mitigation, the CC-VSI works as a grid current-controlling shunt active power filter. Then, the PV array is coupled to the DC bus of the CC-VSI. The MPPT controller employs the Fibonacci search method. The output of MPPT controller is a DC voltage that determines the DC-bus voltage according to the PV maximum power. From computer simulation, the CC-VSI can effectively compensate for harmonics as well as deliver PV power to the grid.**

***Index Terms* — Active Power Filter, MPPT, PV Energy Conversion**.

I. INTRODUCTION

In AC-DC power conversion, a DC side is generally connected to a DC load or, in many applications, a power source such as batteries and photovoltaic panels. On the other hand, an AC side is often an AC load or can be a voltage source from a power utility, or a generator.

In order to control the desired power flow between the DC side and the AC side, a high-frequency switched power converter is usually applied. The power converter (inverter) consists of power semiconductor switches with energy storage devices. The basic popular type of a power converter is a Voltage Source Inverter (VSI) because it is easy to implement, low loss and low cost. Nowadays, power flow control in the VSI (especially for grid connected system) can be achieved using a current-control technique. By controlling the switching instants, the current-controlled VSI (CC-VSI) produces the desired current flow using instantaneous current feedback [1].

A CC-VSI can be used as a shunt active power filter (APF) to improve the power quality of the power system [2-4]. The power converter operates to cancel the harmonics, as well as reactive power from the non-linear loads so that the grid currents will be sinusoidal with unity power factor. The AC side of the CC-VSI attaches to the AC grid at the point of common coupling (PCC) and parallel to the loads, while the DC bus of the CC-VSI contains a DC capacitor.

A CC-VSI can also be applied to transfer active power from a DC source to the AC grid (grid-connected system), as well as to the loads. The AC side of the CC-VSI attaches to the utility grid at the PCC, while the DC side of the CC-VSI is connected to a battery or a renewable energy source such as Photovoltaic system. If connected to solar cells, it is expected that the VSI has the ability to track the maximum power extracted from the PV panels. In literatures [5-7], the power converter operates as a single-stage circuit to achieve directly DC-AC energy transfer with maximum power point tracking (MPPT).

Since the CC-VSI for transferring active power and for canceling harmonics has a similar configuration, it is potential to integrate both functions in one CC-VSI. In this way, the power converter would be able to improve the system power quality as well as to deliver energy from renewable energy sources.

There are few literatures that discuss about combining PV power extraction and active filtering such as in [8-9]. Literature [8] requires calculation of load active power and PV output power to determine the inverter current. Due to switching device safety, power flow of PV power is processed first, while power quality improvement is in the second priority. Moreover, DC-bus controller is used during no insolation. In [9], the current controller requires the measurement of both the load and the inverter currents. The load current is used to calculate the reactive- and harmonic-rich reference value for the inverter current that could create errors and time delays.

This paper proposes a simple and reliable way to integrate active filtering and PV power extracting in one CC-VSI. In addition, the MPPT controller used in this paper is Fibonacci-search-based MPPT. The effectiveness of the MPPT controller and its compatibility with the CC-VSI controller will also be explained. By doing this, the energy efficiency of the system would be significantly increased.

II. THE CC-VSI

The three-phase four-wire CC-VSI for active filter and PV energy extraction is essentially three independent single-phase inverters with a common DC bus. There are inductors at the AC side and a mid-point earthed split capacitor at the DC-bus. It consists of a current control loop to control the harmonic and reactive power and a voltage control loop to control the active power [3-4]. The speed of response of the voltage control loop is much slower than that of the current control loop. Hence, the current control loop and voltage control loop are decoupled.

Moreover, there is a PV array supported by a MPPT controller, which is coupled to the DC-bus of the CC-VSI. Fig. 1 shows the proposed CC-VSI configuration.

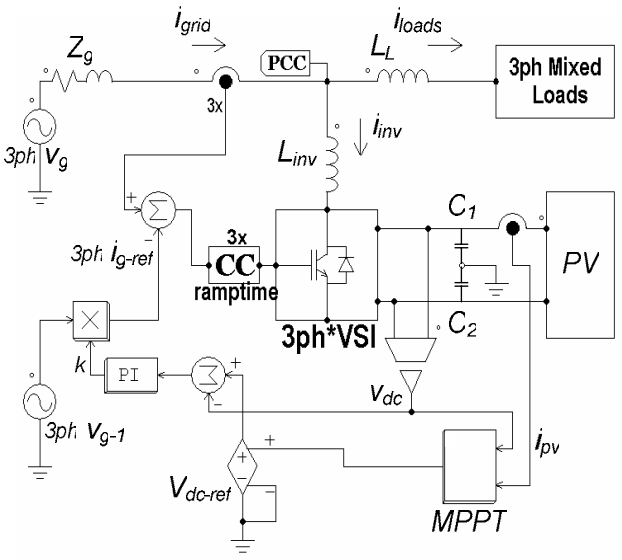

Fig. 1. The proposed CC-VSI configuration

A. Current Control Loop

The current control loop shapes the grid currents, rather than VSI currents, to be sinusoidal and in-phase with the grid voltages by generating a certain pattern of bipolar PWM for continuous switching of the power converter switches according to a ramptime current control technique.

The ramptime current control (RCC) technique has been established as described in the literature [1][12][13]. The principle operation of RCC is similar to a sliding mode control and based on the concept of zero average current error (ZACE). The current error signal is forced to have an average value equal to zero with a constant switching frequency. The RCC maintains the area of positive current error signal excursions equal to the area of negative current error signal excursions, resulting in the average value of the current error signal being zero over a switching period (Fig. 2). The switching period (or frequency) is also kept constant based on the choice of switching instants relative to the zero crossing times of the current error signal. The RCC has a high bandwidth with a fast transient response that can quickly follow the rapid changes in non linear loads.

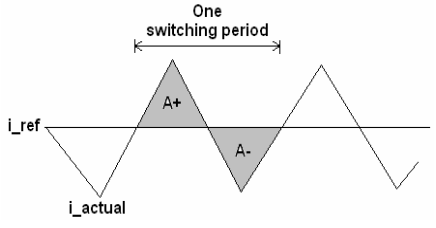

Fig. 2. Zero average current error (ZACE)

In this case, the current sensors are located on the grid side. The grid currents are sensed and directly controlled to follow symmetrical sinusoidal reference signals ($i_{g\text{-}ref}$), which is in-phase with the grid voltages. The reference signal waveform is the same as the fundamental component of the grid voltage, which is obtained using a phase-lock-loop (PLL) circuit. Hence, the outputs of the sensors are compared to the reference signals. The current error signals, which are the difference between the actual currents (grid currents – i_{grid}) and the reference signals – $i_{g\text{-}ref}$, are processed using ramptime current control to generate PWM signals for driving the power switches. Therefore, by forcing the grid currents to be identical to the reference signals, the CC-VSI operates as a shunt active power filter (APF) and automatically provides the harmonic, reactive, negative- and zero-sequence currents for the load according to the basic current summation rule (1) without measuring and determining the unwanted load current components.

$$i_{grid} = i_{inv} + i_{loads} \tag{1}$$

B. Voltage Control Loop

The voltage control loop is a simple Proportional Integral (PI) control to keep the DC-bus voltage at the reference voltage level ($V_{dc\text{-}ref}$) and to provide the amplitude of grid currents. In the voltage control loop, the active power is maintained balanced among the grid, the load and the VSI.

If active power unbalance occurs in the system, there is a voltage deviation (ΔV_{dc}) in the DC bus relative to the reference voltage. For perfect tracking in the current control loop, the voltage control loop responds to adjust the amplitude of grid currents appropriately by adjusting the amplitude of $i_{g\text{-}ref}$ as well as to recover the DC-bus voltage to the reference voltage level. The output of the PI controller, which is a gain k, can determine the amount of ΔV_{dc} that corresponds to the grid current amplitude. The average DC-bus voltage is then recovered and stays at the reference voltage. New steady state active power balance has been achieved with new grid current amplitude. The sinusoidal grid current reference signal is given by

$$i_{g\text{-}ref} = k\, v_{g\text{-}1} \tag{2}$$

where $v_{g\text{-}1}$ is the fundamental component of the grid voltage obtained from a PLL circuit. The value of k is the output of the PI controller. This is an effective way of determining the required magnitude of the grid current, since any mismatch between the required load active power and that being forced by the CC-VSI would result in the necessary corrections to regulate the DC-bus voltage.

III. PV Energy Conversion

The CC-VSI configuration in Fig. 1 has a capability to deliver the solar energy to the AC grid. PV arrays are coupled to the DC bus and parallel to DC-bus capacitors (C_1 and C_2). The amount of active power injected from PV panels is determined by the PV output voltage, which is equal to the DC bus voltage (v_{dc}). For PV array with 1 parallel string and 25

series modules per string, the *p-v* curve of Fuji Electric PV modules (ELR-615-160Z) for several levels of irradiance is shown in Fig. 3. The fluctuation of solar irradiation leads to the variation of PV output power.

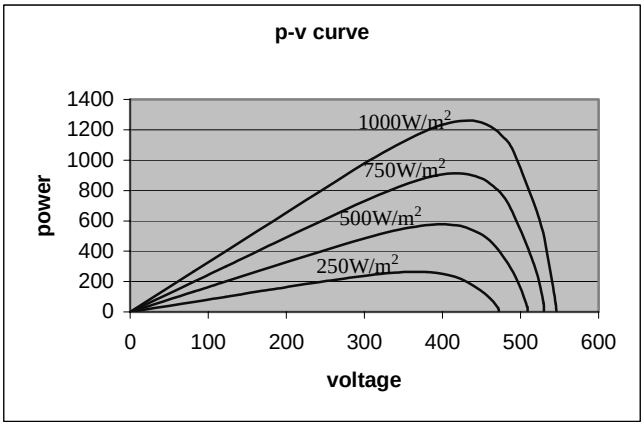

Fig. 3. *p-v* curves of the PV array

The PV modules have to be arranged in an array such that the PV output voltage has to be greater than twice of the peak value of the grid voltage [10]. Otherwise, the CC-VSI is unstable and unable to deliver currents to the grid. On the other hand, there is an upper limit to satisfy voltage insulation requirements of power electronic components.

In addition, there is a MPPT control circuit as a part of the PV system. The objective of the MPPT controller is to set up the DC-bus reference voltage ($V_{dc\text{-}ref}$) corresponding to the PV maximum power. The inputs of the MPPT controller are the output voltage and current of the PV panels. As mentioned before, the voltage control loop will maintain the DC-bus voltage at the reference voltage level. If the DC-bus voltage reaches the reference voltage, the PV output power will be at maximum. At the same time, the active power balance among the grid, the load and the PV panels connected to the DC-bus occurs. The active power of the loads is supplied from the grid and the PV maximum power injection. Thus, the MPPT controller is independent on the current control loop and the voltage control loop of the CC-VSI because it works outside both control loops and simply focuses on setting up the DC-bus reference voltage. The fluctuation of solar irradiation leads to the variation of the DC-bus reference voltage to obtain the PV maximum power.

IV. Fibonacci Search-Based MPPT

The MPPT controller employs the line search method [11]. This method iteratively restricts and shifts the searching range so as to obtain optimal point in the range. The direction of the shift is decided by the value of a function at two points in the range. Fig. 4 is used as an example of the process of restricting and shifting.

Fibonacci sequence, which is represented by (3) is used for setting the length of the range.

$$\begin{aligned} c_{n+2} &= c_{n+1} + c_n \quad (n = 1, 2, ...) \\ c_1 &= c_2 = 1 \end{aligned} \tag{3}$$

The sequence is calculated as

$$c_3 = 2,\ c_4 = 3,\ c_5 = 5,\ c_6 = 8,\ c_7 = 13,\ \ldots \tag{4}$$

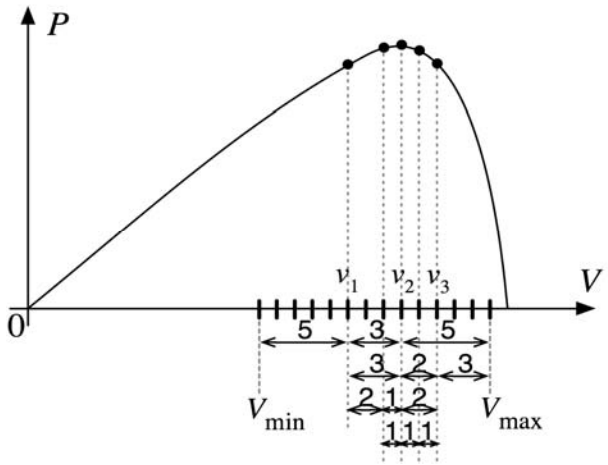

Fig. 4. Searching process

Fig. 4 shows a given *p-v* curve of the PV panel on the interval [V_{min}, V_{max}] to search for maximum power. Two of the interior points v_1 and v_2 are selected to evaluate the function f(v) (= P). Variable v is considered as the DC-bus reference voltage and f(v) can be regarded as the PV output power. If f(v_1) < f(v_2), then the maximum point must occur in the subinterval [v_1, V_{max}]; and we replace $v_1 = V_{min}$ and $V_{max} = V_{max}$, and continue the search in the new subinterval [v_1, V_{max}]. If f(v_1) > f(v_2), then the maximum point must occur in the subinterval [V_{min}, v_2]; and we replace $V_{min} = V_{min}$ and $v_2 = V_{max}$, and continue the search in the new subinterval [V_{min}, v_2]. It is obvious from the figure that f(v_1) < f(v_2). Consequently, the new subinterval is shifted to [v_1, V_{max}] for the next iteration, and the new two interior points (v_2 and v_3) will be selected to evaluate the function f(v).

From Fig. 4, the length of the range, which is determined by Fibonacci sequence in the interval [V_{min}, V_{max}] are expressed as

$$\begin{aligned} [V_{min}, v_1] = [v_2, V_{max}] = a_i = c_n, \\ [v_1, v_2] = b_i = c_{n-1} \end{aligned} \tag{5}$$

The value of a_{i+1} and b_{i+1} can be decided for the next iteration as

$$a_{i+1} = c_{n-1}\ (= b_i),\ b_{i+1} = c_{n-2} \tag{6}$$

Hence, from Fig. 4, numbers on the bottom of the *p-v* curve represent Fibonacci sequence as the length of the range. Any value of n can be selected as a starting point (a_1). In this example, it is chosen to start from $n = 5$ and $c_5 = 5$. It can be seen that the search comes to the convergence when variable n becomes one. At each iteration, the length of the interval narrows according to Fibonacci sequence.

Application of the tracking process to the circuit shown in Fig. 1 will be generally as follows:

1. set $V_{dc\text{-}ref} = v_1$
2. if DC-bus voltage (V_{dc}) = v_1, due to the voltage control loop, then measure PV output power f(v_1)
3. set $V_{dc\text{-}ref} = v_2$
4. if DC-bus voltage (V_{dc}) = v_2, then measure PV output power f(v_2)
5. compare f(v_1) and f(v_2), whether f(v_1) > f(v_2) or f(v_1) < f(v_2)
6. shifting and restricting
7. return to 1 with a new $V_{dc\text{-}ref}$.

As mentioned before, the DC-bus voltage range is limited due to system stability and device insulation requirements, which is in this case in between 376V (V_{min}) and 441V (V_{max}). Outside the limit, Fibonacci search will not be able to find the MPP.

To search the maximum power point (MPP), the Fibonacci sequence may shift to the reverse direction. The MPP may move to be outside of the search range due to a sudden change of insolation. In this case, the search range is being widening. This is realized by reversing the process in Fig. 4. The widening process is practically implemented when the range is shifted to the same direction more than M times and the Fibonacci sequence has not reached the last term c_n. For the next iteration, the value of a_{i+1} and b_{i+1} will be

$$a_{i+1} = c_{n+1}, \quad b_{i+1} = c_n \, (= a_i) \tag{7}$$

V. Simulation Results

The system shown Fig. 1 is examined using computer simulation (PSIM®) to verify the concepts. Table 1 describes the parameter values for the system. The three-phase grid voltages contain harmonics (THD_V = 3.9%), and the mixed loads consist of single- and three-phase linear and non-linear loads (Fig. 5). The characteristics of the PV modules have been represented in Fig. 3.

TABLE 1
Parameter Values For The System Under Study

Symbol	Description	Value
v_g	AC grid voltage, line-line, *rms*	207 V
f	AC line/grid frequency	50 Hz
L_L	Series inductor	0.92 mH
V_{dc}	DC-bus voltage (minimum)	376 V
$C_1 = C_2$	DC Capacitors, electrolytic type	4000 μF
L_{inv}	Inverter inductor	1.52 mH
f_{sw}	Target switching frequency	15.6 kHz

As soon as the system starts, the MPPT controller iteratively limits and shifts the searching range with Fibonacci sequence as the length of the range. In this simulation, a_1 starts with n = 5 and c_5 = 5. The Fibonacci search procedure follows the rule as explained according to Fig. 4. For widening process, the value of M is 2. Fig. 6 depicts the PV output voltage, which equals to the DC-bus voltage and PV output power in steady state for insolation of 0.8kW/m^2. The system converges but oscillates around the maximum power point since the searching process still continues around n = 1. It can be seen that the DC-bus reference voltage, which equals to the output of the MPPT controller is a square wave. The voltage band of the square wave is twice of per-unit length of the range. In this simulation, the voltage per-unit length is 5V. The oscillation may lead to the problem of sub-harmonics to the power system. The voltage band can be reduced by increasing the value of n as a starting point (a_1). As a result, the voltage per-unit length decreases. However, it could increase the transient time. Fig. 6 also shows that the PV output voltage can follow the reference voltage due to the voltage control loop. The average PV output voltage as well as its corresponding average maximum power matches with the insolation level according to Fig. 3. Hence, the Fibonacci-search-based MPPT controller and the voltage control loop work properly to search for the maximum PV output power and to deliver the power to the system.

Fig. 7 illustrates the load current and grid current in phase A. It is obvious that the grid current is smaller than the load current. The load active power is supplied by the grid and the maximum power extracted from the PV array. The active power balance occurs among the grid, the load and the CC-VSI along with PV panels due to the voltage control loop. Moreover, Fig. 7 shows that in spite of oscillation, the grid currents are sinusoidal, balanced and in-phase with the grid voltages due to active filtering operation. It means that the current control loop controls the harmonic and reactive power. Hence, both the current and voltage control loop operates correctly.

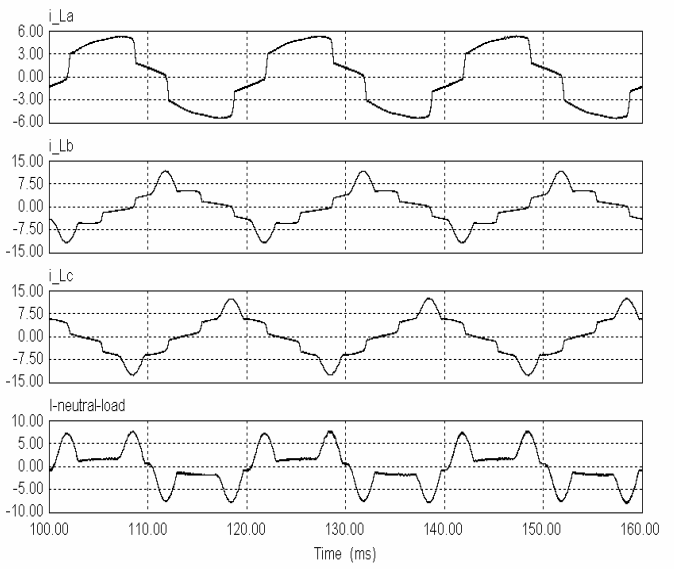

Fig. 5. Mixed-load currents (phase a-b-c-neutral)

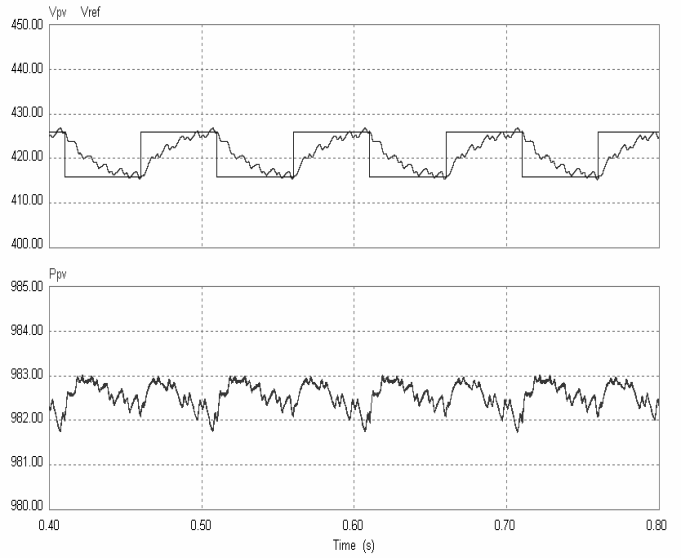

Fig. 6. PV output voltage and its reference (square wave) (top); PV output power (bottom)

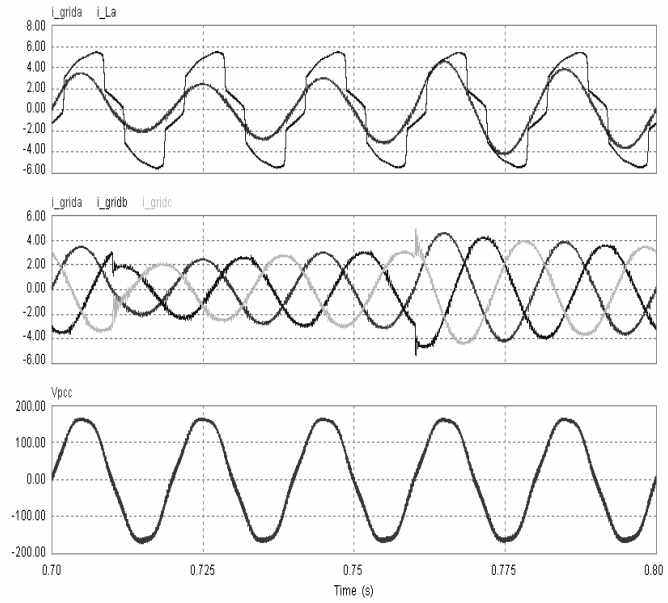

Fig. 7. (top to bottom) the grid and the load currents (phase A); three-phase grid currents; the grid voltage (phase A)

When the irradiation level is below 0.3kW/m^2, the DC-bus voltage is clamped to 376V (V_{min}) due to the stability requirement. As a result, the MPPT controller would function improperly and the maximum PV output power could not be obtained. Fig. 8 demonstrates the grid and the load currents in phase A under zero insolation level. The PV panels do not supply any power and the grid totally supports the load active power. The CC-VSI simply works as a shunt active power filter. Hence, it proves that both control loops can perform independently from the MPPT controller.

Fig. 9 shows the PV output voltage and power as well as the grid current when the insolation is changed, in this case from 0.7kW/m^2 to 0.55kW/m^2. The MPPT controller responds correctly by widening the range to search another MPP. Then, the searching process continues as usual by narrowing the range to obtain the new MPP. It can be seen from Fig. 9 that the PV output voltage and power decrease. As a result, the grid current increase because the PV power delivered to the load decreases.

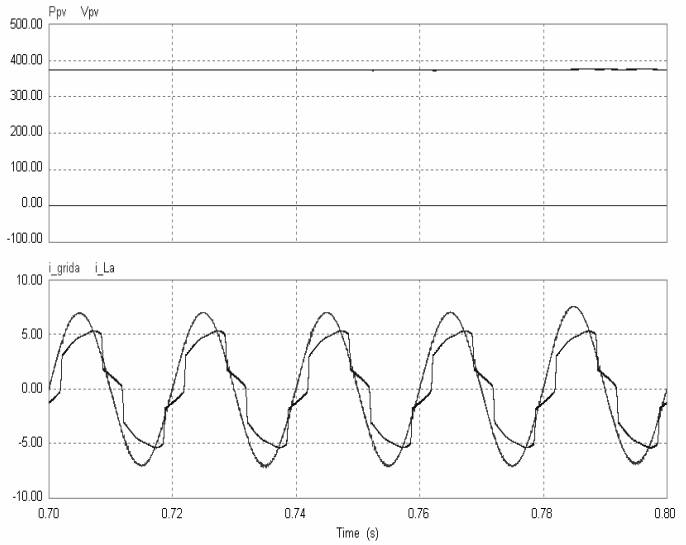

Fig. 8. PV output voltage and power under zero insolation level (top); the grid and the load currents – phase A (bottom)

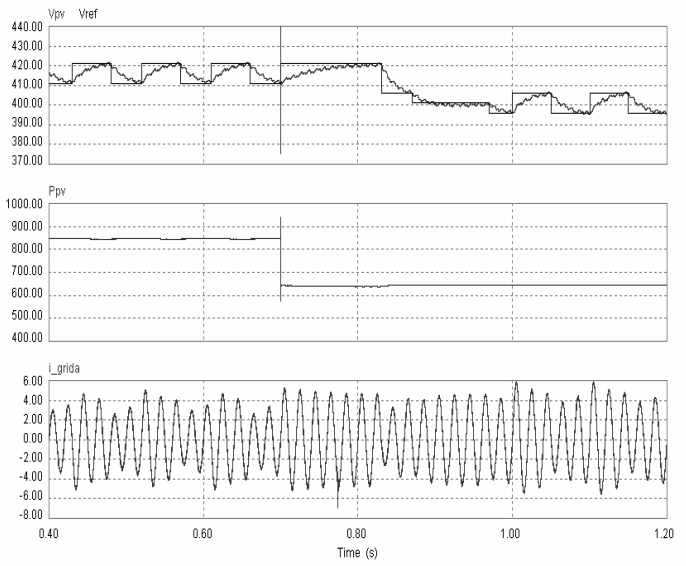

Fig. 9. When the insolation is changed (0.7kW/m^2 to 0.55kW/m^2) (top to bottom): PV output voltage (and its reference); PV output power; the grid current (phase A)

VI. CONCLUSION

This paper describes the capability of a CC-VSI for active filtering and PV energy extraction. From simulation results, in steady state and dynamic condition, it proves that both

harmonic and reactive power mitigation and PV energy extraction can be integrated effectively in one CC-VSI. The control strategy using the current control loop and the voltage control loop can handle both functions simultaneously. The system is stable and reliable. The current control loop directly shapes the grid currents to be sinusoidal and in-phase with the grid voltages, while the voltage control loop maintains the DC-bus voltage constant and regulates the active power balance among the grid, the load and the CC-VSI supported by PV panels. The load power is supplied by the grid power and the PV power. At the same time, in spite of PV output voltage oscillation, the Fibonacci-search-based MPPT controller effectively and independently searches for the PV maximum power. As a result, the energy efficiency of the system will be increased significantly.

REFERENCES

[1] Borle, L., "Zero Average Current Error Control Methods for Bidirectional AC-DC Converters", PhD Thesis, 1999, Electrical and Computer Engineering, Curtin University of Technology, Western Australia

[2] El-Habrouk, M., M.K. Darwish, and P. Mehta, "Active power filters: a review", *Electric Power Applications, IEE Proceedings*-, 2000. **147**(5): p. 403-413.

[3] Tumbelaka, H.H., L.J. Borle, and C.V. Nayar, "Analysis of a Series Inductance Implementation on a Three-phase Shunt Active Power Filter for Various Types of Non-linear Loads", *Australian Journal of Electrical and Electronics Engineering, Engineers Australia*, 2005. **2**(3): p. 223-232.

[4] Tumbelaka, H.H., L.J. Borle, C.V. Nayar, and S.R.Lee, "A Grid Current-controlling Shunt Active Power Filter", *Journal of Power Electronics*, vol. 9, no. 3, 2009, p. 365-376.

[5] Chen, Y., and Smedley, K.M., "A Cost-Effective Single-State Inverter with Maximum Power Point Tracking", *IEEE Transactions on Power Electronics*, 2004, 19(5): p. 1289-1294.

[6] Castaner, L., and Silvestre, S., "Modelling Photovoltaic System using PSpice", John Wiley & Sons, 2002.

[7] Wanzeller, M.G. et.al., "Current Control Loop for Tracking of Maximum Power Point Supplied for Photovoltaic Array", *IEEE Transactions on Instrumentation and Measurement*, 2004, 53(4): p. 1304-1310.

[8] Wu, Tsai-Fu et.al., "PV Power Injection and Active Power Filtering with Amplitude-Clamping and Amplitude-Scaling Algorithms", *IEEE Trans. on Industry Application*, 2007, **43**(3): p.731-741

[9] Grandi, G., Casadei, D., and Rossi, C., "Direct Coupling of Power Active Filters with Photovoltaic Generation System with Improved MPPT Capability", *in IEEE Power Tech Conference*, 2003. Bologna, Italy.

[10] Tumbelaka, H.H., L.J. Borle, and C.V. Nayar, "A New Approach to Stability Limit Analysis of A Shunt Active Power Filter with Mixed Non-linear Loads", *in Australasian Universities Power Engineering Conference (AUPEC)*. 2004. Brisbane, Australia: ACPE. p. ID: 121

[11] Ahmed, N.A, and Miyatake, M., "A Novel Maximum Power Point Tracking for Photovoltaic Applications under Partially Shaded Insolation Conditions", *Electric Power System Research*, 2008, **78**(5), p. 777-784.

[12] L. J. Borle, and C. V. Nayar, "Ramptime Current Control", *in Conf. Proc. 1996 IEEE Applied Power Electronics Conference (APEC'96)*, p. 828-834.

[13] L. J. Borle, and C. V. Nayar, "Zero Average Current Error Controlled Power Flow for AC-DC Power Converter", *IEEE Trans. on Power Electronics*, **10**(1): pp. 725-732. 1995.